Materials Letters 70 (2012) 167–170

Contents lists available at SciVerse ScienceDirect

Materials Letters

journal homepage: www.elsevier.com/locate/matlet

Dimensional effects on the structure and magnetic properties of $GdMnO_3$ thin films

Y. Romaguera-Barcelay [a,b], J. Agostinho Moreira [a,*], A. Almeida [a], J.P. Araújo [a], J. Pérez de la Cruz [b]

[a] IFIMUP and IN-Institute of Nanoscience and Nanotechnology, Departamento de Física e Astronomia, Faculdade de Ciências da Universidade do Porto, Rua do Campo Alegre, 687, 4169-007 Porto, Portugal
[b] INESC Porto, Rua do Campo Alegre, 687, 4169-007 Porto, Portugal

ARTICLE INFO

Article history:
Received 11 November 2011
Accepted 3 December 2011
Available online xxxx

Keywords:
Multiferroic
Thin films
Dimensional effect

ABSTRACT

This work is addressed to studying $GdMnO_3$ thin films, prepared by a chemical solution method on oriented Pt substrates. Alterations regarding structure and magnetic response of both ceramics and single crystals show that the behaviour of the as-prepared films can be understood by assuming a continuously changing of the in-plane stress state in the film induced by mechanical coupling with the substrate. The emerging of a ferromagnetic response in the thin films is a consequence of the structural deformations induced by matching both film and substrate during the growth process, which alters the balance between competitive antiferromagnetic and ferromagnetic interactions.

Recent advances in thin films growth techniques have enabled to prepare a large variety of heterostructures consisting of materials with different crystal structures and physical properties [1]. In particular, the research on the application of magnetoelectric materials as barriers and interfaces for spintronic has known a very large increase. Moreover, the low dimensionality and size required for such devices can yield drastic changes onto both structure and physical properties of the bulk materials, largely due to substrate-induced structural deformations [2,3].

Among the magnetoelectric materials, $GdMnO_3$ has been intensively studied as this material exhibits magnetic-induced ferroelectricity. The crystal structure of $GdMnO_3$ at room temperature is described by the P*bnm* space group [4]. The Mn^{3+} magnetic momenta presumably order incommensurately below $T_N = 43$ K, and turning between 16 and 23 K into a canted A-type antiferromagnetic structure, with weak ferromagnetic character, polarizing the Gd 4f spins [4,5]. On further cooling, the weak ferromagnetic component keeps evolving, and at 6.5 K, due to the interaction of the 4f spins, long-range order of the Gd moment occurs [4,5]. A canting of the Gd spins turns up with a ferromagnetic component antiparallel to the ferromagnetic moment of the canted Mn spins [4]. The magnetic-induced ferroelectric phase for **H**//**b** has been associated with a specific ordering of the Gd^{3+} momenta, likely stabilizing a cycloidally modulated Mn^{3+} momenta ordering [4,5].

In this work we present an experimental study regarding the influence of the substrate/film matching on the structure and magnetic properties of $GdMnO_3$ thin films.

$GdMnO_3$ thin films used in this work were processed through a chemical solution method, described in Ref. [6], and sintered at 800 °C. The crystal structure, morphology and roughness of the as-processed $GdMnO_3$ thin films were analyzed by X-ray diffraction, scanning electron microscopy, and atomic force microscopy. No secondary chemical and crystallographic phases were detected. Scanning electron microscopy data revealed a smooth surface, presenting a well-defined grain structure. The average film thickness was calculated from a cross-section scanning electron microscopy analysis. We have chosen to prepare 38 nm, 108 nm and 180 nm thick films. The analysis of the energy dispersive X-ray spectra revealed the expected 1:1 Gd/Mn ratio, according to the $GdMnO_3$ formula. By investigating the X-ray pattern of the films through a profile matching, an orthorhombic metric appears as a good candidate. Within experimental resolution, X-ray spectra yield the P*bnm* space group, with the [121] preferential orientation. The cell parameters obtained from profile matching analysis of the X-ray pattern recorded in the 180 nm thick film are $a = 5.800(2)$ Å, $b = 7.384(1)$ Å, and $c = 5.332(1)$ Å. The a and b parameters are about 1% less, while c is 0.4% larger than the respective values obtained in single crystals and ceramics [7].

The unpolarized Raman spectra of the sintered $GdMnO_3$ thin films at room temperature were obtained with a Jobin-Yvon T64000 spectrometer working in subtractive mode and detected with a charge-coupled device. The holographic gratings were kept in the same position for all the recorded spectra. The spectral slit width was about 1.5 cm^{-1}. Raman spectra of the as-processed films, as well as, of a ceramic sample are shown in Fig. 1(a), in the frequency range 180–800 cm^{-1}.

In $GdMnO_3$ single crystals, the A_g and B_{2g} Raman bands are the most intense, and they are used for the mode assignment presented further below in this work. Despite the absence of anisotropy in the as-processed films, due to their polycrystalline nature, ruling out mode

---

* Corresponding author.
E-mail address: jamoreir@fc.up.pt (J.A. Moreira).

doi:10.1016/j.matlet.2011.12.018

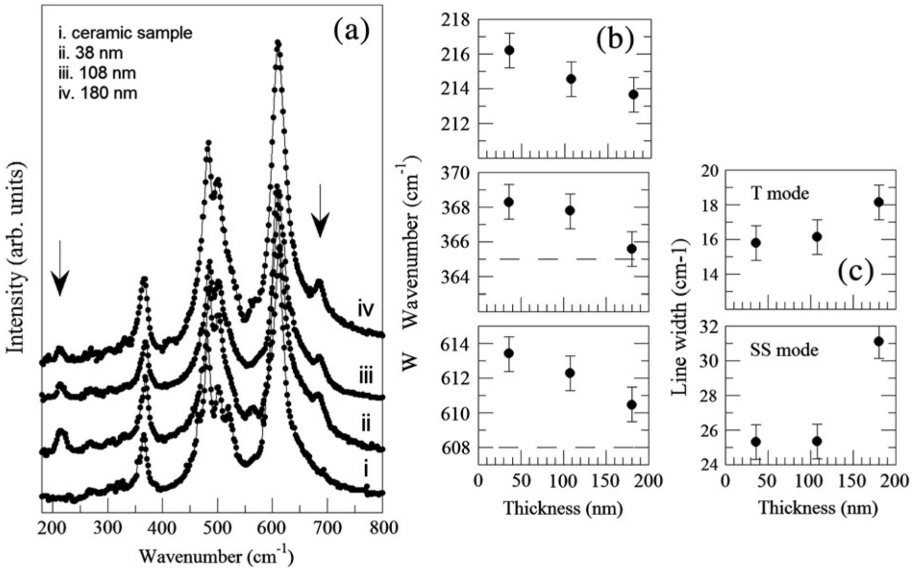

Fig. 1. (a) Raman spectra of $GdMnO_3$ ceramic (i), and 38 nm (ii), 108 nm (iii), and 180 nm (iv) thick $GdMnO_3$ films, recorded at room temperature. (b) Frequency and (c) bandwidth of some selected Raman bands versus film thickness. The horizontal dashed lines correspond to the values obtained in bulk samples.

assignment by considering extinction rules, a confident mode assignment can be still reached by comparing relative intensities of these modes.

In the 350–650 cm^{-1} range, several strong bands can be observed, whose assignment is straightforward if we take into account the data reported in Ref. [8]. Thus, the band at 614 cm^{-1} is associated with the symmetric stretching (SS) mode involving the equatorial oxygen atoms (symmetry B_{2g}), the band at 508 cm^{-1} to the bending mode (symmetry B_{2g}), the band at 485 cm^{-1} to the Jahn-Teller type asymmetric stretching mode involving also the equatorial oxygen atoms (symmetry A_g), and the band at 368 cm^{-1} to the lattice (T) mode involving the tilt of the MnO_6 octahedra (symmetry A_g). These bands are compatible with the P*bnm* symmetry, evidenced from analysis of the X-ray patterns. Other bands observed in thin films are not. This is the case of the bands located at 214 and 685 cm^{-1} (signalized in Fig. 1(a) with arrows), as well as, the weak bands arising at 413 and 577 cm^{-1}. As no bands were observed in the Raman spectrum of a thermally treated substrate, their existence is likely due to some kind of mechanical deformation in the film, induced close to the film/substrate interface, through mechanical clamping. This assumption is supported by the behaviour of the frequency and line width of the Raman bands with increasing film thickness. Fig. 1(b) and (c) show, respectively, the film thickness dependence of the frequency and line width of some representative Raman bands. As the thickness increases the frequency of Raman bands decreases towards the value in ceramics and single crystals. Furthermore, the bandwidth of lattice T and internal SS modes increases with film thickness.

These results are straightforward understood if we consider the existence of a stressed low-lying portion in all films and stress gradient in the perpendicular direction to the film surface. Since the cell parameters of the Pt substrate are smaller than the cell parameters of $GdMnO_3$, during deposition, the substrate molecular interactions force the film into the substrate crystal symmetry. This effect is more pronounced in the film portion close to the substrate, since stress is expected to be higher in this region. Thus, away from the substrate/film interface, the portion of the film with a thickness of some nanometres less than the film has an orthorhombic P*bnm* structure confirmed by the Raman signature referred to above. Contrarily, the low-lying portion of the film in contact with the substrate surface has a lower symmetry enforced by mechanical matching between the P*bnm* structure and the F*m–3m* of the substrate. The symmetry lowering is distinctive marked by the emerging new bands observed in the Raman spectra of the film. The stress gradient normal to the film surface is supported by the width increase of Raman bands. In fact, as the scatter volume is enlarging from the interface substrate/film towards the film surface, the oscillators frequency decreases continuously. So, each Raman band arises from a continuous distribution of several oscillators, whose frequency takes values in a narrow spectral range, less than the available spectral resolution. This is the reason why the bandwidth increases with increasing film thickness.

If it is assumed the existence of a stress gradient in the $GdMnO_3$ film, this feature will be ascertained from the study of its physical properties, in particular of its magnetic behaviour. In fact, early works [10] evidenced that distorting the $GdMnO_3$ crystalline structure may change the Mn–O–Mn bond angle, which then critically alters the balance between the competing ferromagnetic and antiferromagnetic interactions.

Thus, we have measured the low-field (100 Oe) induced magnetization in zero-field (ZFC) and field (FC) cooling conditions, as a function of temperature, shown in Fig. 2, and the magnetization as a function of the magnetic field strength, M(H), up to ± 50 kOe, measured at several fixed temperatures for the 38 and 180 nm thick films

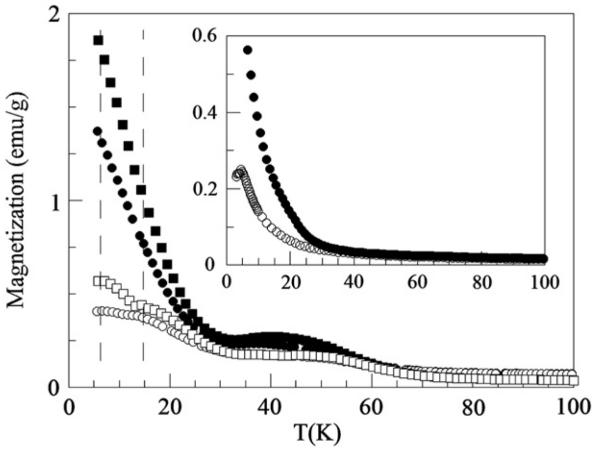

Fig. 2. Temperature dependence of the specific magnetization of $GdMnO_3$ 38 nm (circles) and 180 nm (squares) thick films, measured in ZFC (open markers) and FC conditions (closed markers). The inset shows the low-field magnetization measured for the same experimental conditions, in a $GdMnO_3$ ceramic.

(see Fig. 3). For these measurements we have used a SQUID magnetometer, with precision of 10^{-7} emu. The magnetic response of substrate was also measured, and no abnormal temperature behaviour was observed.

Above 80 K, both ZFC and FC induced magnetizations merge together, steadily increasing with decreasing temperatures. Opposed to the behaviour obtained in the $GdMnO_3$ ceramics, the magnetization of the $GdMnO_3$ thin films does not follow a Curie–Weiss law [4]. Below 70 K, the ZFC and FC magnetization curves become distinct, marking the upper temperature limit of magnetic ordering in the $GdMnO_3$ films. It is worth stressing that the corresponding temperature, $T_1 = 70$ K, obtained in both $GdMnO_3$ films is ~30 K higher than the values referred to for the Nèel temperature of both single crystals and ceramics [4].

Just below T_1, within the temperature range of the incommensurate phase observed for bulk samples, rather unexpected issues regarding films' magnetic behaviour can be sorted out. Firstly, a broad anomaly in the temperature dependence of both ZFC and FC magnetizations is observed in the 35–60 K temperature range. Secondly, ferromagnetic hysteretic cycles are also observed inside this phase, as it is shows in Fig. 3(b) and (e). The ferromagnetic ordering emerging in this phase evidences both the loss of the incommensurate collinear sinusoidal spin arrangement, and the strengthening of the FM super-exchange interactions over the AFM ones.

Another magnetic phase transition is well marked by an anomalous behaviour of ZFC curve and a slightly change of slope of the FC curve at around $T_2 = 17$ K, as shown in Fig. 2. The ZFC curve also exhibits an anomaly at 7 K, associated with the ordering of Gd^{3+} spins. Below T_2, ferromagnetic hysteresis loops were obtained, as shown in Fig. 3, also evidencing the existence of FM ordering in the two lowest magnetic phases.

The effect of film thickness on the magnetic properties can be evidenced from the value of the saturation magnetization (Ms), obtained from M(H) cycles at high fields, and from the temperature dependence of the remnant magnetization (Mr), ascertained from the crossing of the M(H) curves with the magnetization axis. Mr(T) data are presented in Fig. 4. While Ms values obtained for the 180 nm thick film agrees with the ones reported for single crystals [5] and nanoparticles [9], for the thinner film, Ms is about 1 order of magnitude lower. In both films, Mr(T) decreases as temperature increases. However, for the thinner film, Mr keeps non-zero values up to 70 K, while for the thicker film, Mr vanishes above 50 K. The

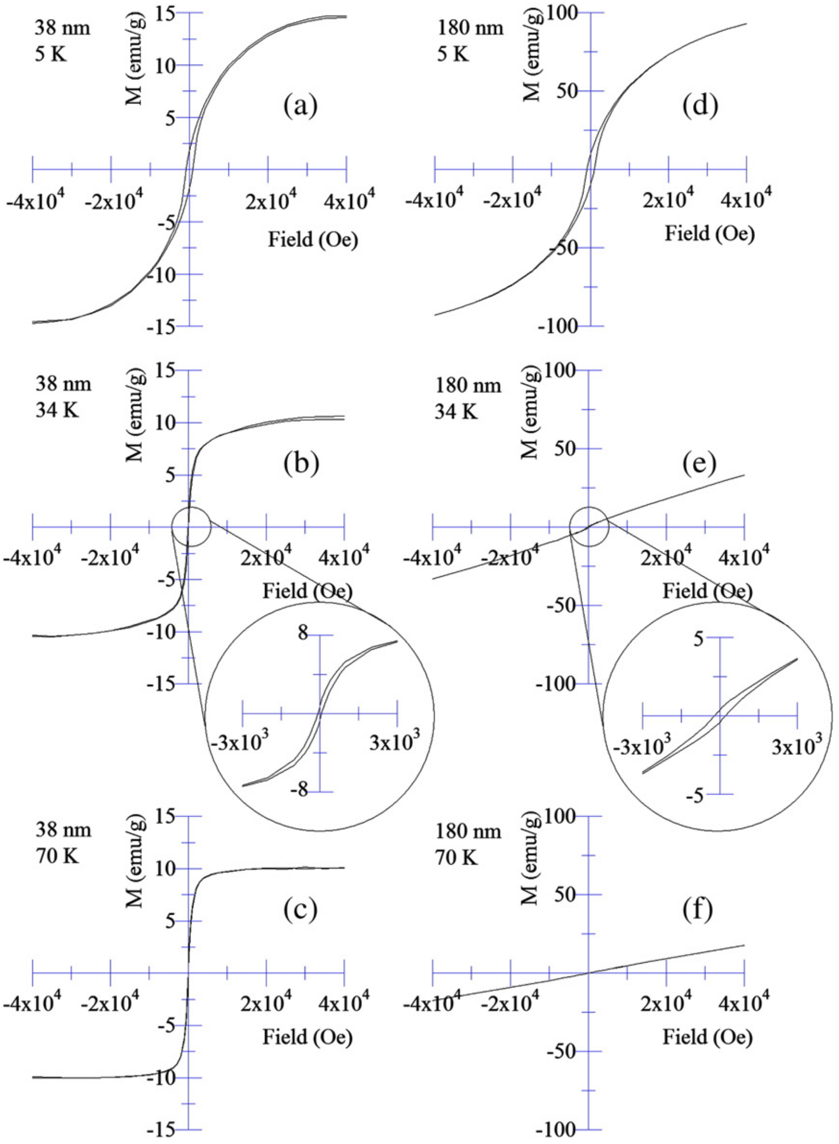

Fig. 3. M(H) relations of $GdMnO_3$ 38 nm and 180 nm films, at fixed selected temperatures.

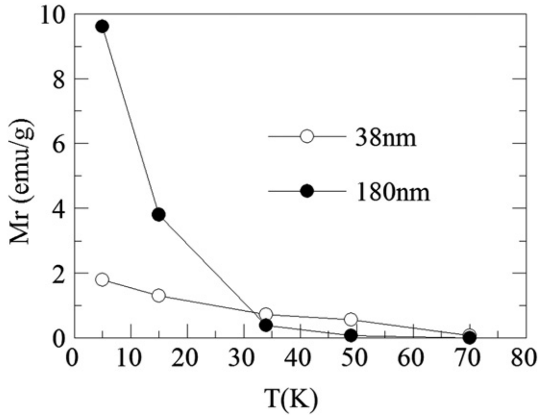

Fig. 4. Temperature dependence of the remnant magnetization of $GdMnO_3$ 38 nm and 180 nm thick films.

Mr(T) curve does not follow the classical temperature dependence foreseen by the mean-field approach, eventually due to the high paramagnetic susceptibility of the Gd^{3+} ions.

Some of the aforementioned results diverge from those obtained in single crystals and ceramics [4,5]. As an example, the inset of Fig. 2 shows the low-field magnetization measured for the same experimental conditions, in a $GdMnO_3$ ceramic. As it can be seen, the ZFC and FC curves merge above $T_N = 42$ K, and no anomaly is observed near this temperature. A similar behaviour is found in the temperature dependence of the induced magnetization of single crystals [4]. Moreover, the well-defined anomaly at $T_N = 8$ K in the magnetization curves obtained from bulk samples, appears smeared out in the case of the films, likely due to some magnetic disordering.

Since the results obtained in the films, from both Raman and magnetization studies, are distinctly different from bulk samples, we are led to assign these differences to the existence of a stress gradient, normal to the film surface. In fact, as it was referred to above, Raman spectra exhibit bands coming from the P*bnm* structure, and also other ones, associated with symmetry lowering due to in-plane strains in the portion of the film close to the substrate. These existing strains may induce significant changes in the Mn–O–Mn bond angle, which as it was referred to above has a crucial effect on the balance between the competing ferromagnetic and the antiferromagnetic interactions [10]. Thus, we interpret our results, in particular the ferromagnetic response in the films, as a consequence of the aforesaid mechanism, where the strain-induced changes in Mn–O–Mn bond angle, yields prevailing the FM interactions against the AFM ones.

In summary, this work is addressed to studying high quality $GdMnO_3$ thin films, processed by a chemical solution method on oriented Pt substrates. Alterations regarding lattice dynamic and magnetic response of the films compared to both ceramics and single crystals ascertained through Raman and magnetic studies show that the behaviour of the as-prepared films can be interpreted by assuming a continuously changing of the stress state in the film, induced by the substrate. The emerging of short-range magnetic interactions was also evidenced above T_1, which contributes to the departure of magnetization from following the Curie–Weiss law in the paramagnetic phase.

Acknowledgements

Y. Romaguera thanks the financial support by the Programme Alβan (The European Union Programme of High Level Scholarships for Latin America, scholarship no. E07D401169CU). This work was supported by Fundação para a Ciência e Tecnologia, through the Project PTDC/CTM/099415/2008.

References

[1] Eerenstein W, Mathur ND, Scott JF. Nature (London) 2006;442:759.
[2] Lee J-H, Lee P, Murugavel SY, Jang TW, Noh Y, Jo2 M-H, et al. Appl Phys Lett 2007;90:182504.
[3] Feng W, Van Thiet D, Dung DD, Shin Y, Cho S. J Appl Phys 2010;108:113903.
[4] Kimura T, Lawes G, Goto T, Tokura Y, Ramirez AP. Phys Rev B 2005;71:224425.
[5] Hemberger J, Lobina S, Krug von Nidda H-A, Tristan N, Ivanov VYu, Mukhin AA, et al. Phys Rev B 2004;70:024414.
[6] Romaguera-Barcelay Y, Agostinho Moreira J, González-Aguilar G, Almeida A, Araujo JP, Pérez de la Cruz J. J Electroceram 2011;26:44–55.
[7] Mori T, Kamegashira N, Aoki K, Shishido T, Fukuda T. Mater Lett 2000;54:238.
[8] Iliev MN, Abrashev MV, Laverdière J, Jandl S, Gospodinov MM, Wang YQ, et al. Phys Rev B 2006;73:064302.
[9] Wang XL, Li D, Cui TY, Kharel P, Liu W, Zhang ZD. J Appl Phys 2010;107:09B510.
[10] Mochizuki M, Furukawa N. Phys Rev B 2009;80:134416.